Science in China Series A: Mathematics
Aug., 2008, Vol. 51, No. 8, 1440–1460
www.scichina.com math.scichina.com
www.springerlink.com

Residual-based a posteriori error estimates of nonconforming finite element method for elliptic problems with Dirac delta source terms

DU ShaoHong[1,2] & XIE XiaoPing[1,3†]

[1] School of Mathematics, Sichuan University, Chengdu 610064, China
[2] School of Science, Chongqing Jiaotong University, Chongqiong 400047, China
[3] Yangtze Center of Mathematics, Sichuan University, Chengdu 610064, China
(email: shaohongdu@gmail.com, xpxie@scu.edu.cn)

Abstract Two residual-based a posteriori error estimators of the nonconforming Crouzeix-Raviart element are derived for elliptic problems with Dirac delta source terms. One estimator is shown to be reliable and efficient, which yields global upper and lower bounds for the error in piecewise $W^{1,p}$-seminorm. The other one is proved to give a global upper bound of the error in L^p-norm. By taking the two estimators as refinement indicators, adaptive algorithms are suggested, which are experimentally shown to attain optimal convergence orders.

Keywords: Crouzeix-Raviart element, nonconforming FEM, a posteriori error estimator, longest edge bisection

MSC(2000): 65N15, 65N30, 65N50

1 Introduction and main results

Consider the Poisson problem with the Dirac delta source term and homogeneous Dirichlet boundary condition:

$$\begin{cases} -\triangle u = \delta_{x_0}, & \text{in} \quad \Omega, \\ u = 0, & \text{on} \quad \partial\Omega, \end{cases} \tag{1.1}$$

where $\Omega \subset R^2$ is a bounded polygonal domain and x_0 is an inner point of Ω.

The problem (1.1) arises in some fields such as the electric field generated by a point charge, transport equations for effluent discharge in aquatic media, modeling of acoustic monopoles, etc.

As shown in [1], the weak solution of problem (1.1) belongs to L^p for $p < \infty$ and to $W^{1,p}$ for $p < 2$. In [2, 3], a priori estimates in L^2-norm were given, whereas in [4] interior maximum norm error estimates were proved.

Due to the singular characteristics of the solution of the problem (1.1), meshes adequately refined around the delta support are required to improve the quality of the approximation. To

Received March 12, 2008; accepted May 8, 2008
DOI: 10.1007/s11425-008-0113-0
† Corresponding author
This work was supported in part by the National Natural Science Foundation of China (Grant No. 10771150), the National Basic Research Program of China (Grant No. 2005CB321701), and the Program for New Century Excellent Talents in University (Grant No. NCET-07-0584)

this end, adaptive schemes based on some a posteriori error indicators should be used (see for instance [5, 6]). In the paper [1], a posteriori error analysis for the conforming finite element method was performed for this problem, and a posteriori error estimators were established which yield global upper and local lower bounds in L^p norm and $W^{1,p}$ seminorm, for p ranging on some intervals depending on the geometry of the domain.

A posteriori error analysis of nonconforming finite element (abbr. NFE) approach (see for instance [7–10]), to the authors' knowledge, has not so far been seen for the problem (1.1). So the main purpose of this paper is to derive reliable and efficient a posteriori error estimation of the error in piecewise $W^{1,p}$-seminorm for the nonconforming P_1 triangular element (Crouzeix-Raviart element). The key point in the analysis is to apply a Helmholtz-type decomposition of a function in $L^q(\Omega)^2$ and to follow the routine of dual arguments, where $\frac{1}{p}+\frac{1}{q}=1$. Another task of the paper is to develop a reliable global upper bound of the error in L^p norm.

The problem (1.1) can be written in a weak form: Find $u \in W_0^{1,p}(\Omega)$ such that

$$\int_\Omega \nabla u \cdot \nabla v = \langle \delta_{x_0}, v\rangle, \qquad \forall\, v \in W_0^{1,q}(\Omega), \tag{1.2}$$

with $\frac{1}{p}+\frac{1}{q}=1$. The right-hand side is well defined because, for $q>2$, $W^{1,q}(\Omega)\subset C(\Omega)$.

Let $\mathcal{T}_h$ be a shape-regular triangulation of triangular meshes of the domain Ω (cf. [11]). We denote by $\varepsilon_h, \varepsilon$ the sets of all interior edges and edges, respectively. Let $W_h = \mathrm{CR}_0^1(\mathcal{T}_h)$ be the Crouzeix-Raviart NFE space given by

$$\mathrm{CR}_0^1(\mathcal{T}_h) := \left\{ \begin{array}{l} v_h \in L^q(\Omega) : v_h|_T \in P_1(T), \text{ for all } T \in \mathcal{T}_h;\ v_h \text{ is} \\ \text{continous at the midpoint, mid}(E), \text{ of } E,\ \forall E \in \varepsilon_h; \\ \ v_h(\mathrm{mid}(E)) = 0,\ \forall E \subset \partial\Omega. \end{array} \right\}$$

Details on this element can also be found in [12–14]. Then the NFE method for the problem (1.1) reads as: find $u_h \in W_h$ such that

$$\sum_{T\in\mathcal{T}_h} \int_T \nabla_h u_h \cdot \nabla_h v_h = \int_\Omega \delta_{x_0} v_h, \qquad \forall\, v_h \in W_h. \tag{1.3}$$

Here and in what follows, ∇_h denotes the elementwise gradient (with respect to $\mathcal{T}_h$).

For any $v_h \in W_h$, v_h is continuous at the point x_0 only when x_0 is an inner point of an element or a midpoint of an element edge, and then $\int_\Omega v_h(x)\delta_{x_0} = v_h(x_0)$. When x_0 lies in an interior edge but is not a midpoint, the right-hand side of (1.3) is not well defined, because v_h is not continuous at x_0. In this case, the right-hand side of (1.3) is redefined as

$$\int_\Omega v_h(x)\delta_{x_0} := \frac{1}{k}\sum_{i=1}^{k} v_h|_{T_{0i}}(x_0),$$

where T_{0i} $(1 \leqslant i \leqslant k)$ denote the triangles sharing the point x_0 which is not a midpoint of an interior edge.

Let $E \in \varepsilon_h$ be an interior edge shared by two adjacent elements $T_+, T_- \in \mathcal{T}_h$ (see Figure 1), with length h_E. Let $\boldsymbol{n}_E$ and τ_E be the unit outward normal and tangential vector of E in T_+, respectively. Denote by

$$J_E(u_h) = \left[\frac{\partial u_h}{\partial \boldsymbol{n}_E}\right] := \frac{\partial u_h}{\partial \boldsymbol{n}_E}\bigg|_{T_+} - \frac{\partial u_h}{\partial \boldsymbol{n}_E}\bigg|_{T_-}$$

the jump of flux across E, by $[\nabla_h u_h]_E = \nabla_h u_h|_{T_+} - \nabla_h u_h|_{T_-}$ the jump of the elementwise gradient $\nabla_h u_h$ across E, and by $[u_h]_E := u_h|_{T_+} - u_h|_{T_-}$ the jump of u_h across an interior edge E. For an edge $E \subset \partial\Omega$ and a function $g \in C^1(E)$, $\partial_\varepsilon g$ denotes the edge gradient along E (with respect to a proper Cartesian coordinate system along the flat one dimensional manifold E). Then we say $v|_E \in W^{1,p}(E)$ if v has weak derivatives on E such that

$$\|v\|^p_{W^{1,p}(E)} := \|v\|^p_{0,p,E} + \|\partial_\varepsilon v\|^p_{0,p,E} < \infty$$

(see [15]). In the following, h is understood as a piecewise constant function with $h|_T = h_T = \mathrm{diam}(T)$ and $h|_E = h_E$.

In this paper, the following computable error estimator,

$$\varepsilon_p := \begin{cases} \left\{ \sum_{E\in\varepsilon_h} \|h_E^{\frac{1}{p}}[\nabla_h u_h]_E\|^p_{0,p,E} \right. \\ \qquad \left. + \sum_{E\subset\partial\Omega} \|h_E^{\frac{1}{p}}\nabla_h u_h \cdot \tau_E\|^p_{0,p,E} \right\}^{\frac{1}{p}}, & \text{if } u_h \text{ is continuous at } x_0, \\ \left\{ \sum_{i=1}^{k} \frac{h_{T_{0i}}^{2-p}}{k^p} + \sum_{E\in\varepsilon_h} \|h_E^{\frac{1}{p}}[\nabla_h u_h]_E\|^p_{0,p,E} \right. \\ \qquad \left. + \sum_{E\subset\partial\Omega} \|h_E^{\frac{1}{p}}\nabla_h u_h \cdot \tau_E\|^p_{0,p,E} \right\}^{\frac{1}{p}}, & \text{otherwise}, \end{cases} \tag{1.4}$$

is derived and shown to yield global lower and upper bounds of the error in piecewise $W^{1,p}$-seminorm,

$$\|\nabla_h(u-u_h)\|_{0,p,\Omega} = \left(\sum_{T\in\mathcal{T}_h} |u-u_h|^p_{1,p,T}\right)^{\frac{1}{p}}, \tag{1.5}$$

where in (1.4) k denotes the number of the triangles sharing x_0.

For the error $\|u-u_h\|_{0,p,\Omega}$, a reliable and computable error estimator is also given as

$$\eta_p := \begin{cases} \left\{ \sum_{E\in\varepsilon_h} (h_E^{p+2}|J_E(u_h)|^p + h_E\|[u_h]_E\|^p_{0,p,E}) \right. \\ \qquad \left. + \sum_{E\subset\partial\Omega} h_E^{1+p}\|\partial\varepsilon u_h\|^p_{0,p,E} \right\}^{\frac{1}{p}}, & \text{if } u_h \text{ is continuous at } x_0, \\ \left\{ \sum_{i=1}^{k} \frac{h_{T_{0i}}^{2}}{k^p} + \sum_{E\in\varepsilon_h} (h_E^{p+2}|J_E(u_h)|^p \right. \\ \qquad \left. + h_E \| [u_h]_E \|^p_{0,p,E}) + \sum_{E\subset\partial\Omega} h_E^{1+p}\|\partial\varepsilon u_h\|^p_{0,p,E} \right\}^{\frac{1}{p}}, & \text{otherwise}. \end{cases} \tag{1.6}$$

The above two a posteriori error estimators, ε_p and η_p, are served as refinement indicators to guide adaptive mesh-refining algorithms, which are based on the bulk criterion for displacement-based adaptive finite element methods[16–18] and the longest-edge bisection. For details on the longest-edge bisection and corresponding data handling, we refer to [19–22]. For corresponding details on the Laplace equation, one can see [23–31]. Numerical experiments show that the adaptive algorithms proposed in this paper have optimal convergence orders.

The remaining part of this paper is arranged as follows: In Section 2 some Preliminary results are provided. Section 3 is devoted to the proof of equivalence of the error estimator ε_p and the error in piecewise $W^{1,p}$ seminorm. In Section 4 the estimator η_p is shown to be a reliable global upper bound of the error in L^p norm. Some numerical results are reported in Section 5 to verify the performance of the adaptive algorithm. Conclusions are made in the finial section.

2 Notations and preliminaries

Throughout the rest of the paper the notation $A \lesssim B$ represents $A \leqslant CB$ with a mesh-size independent constant $C > 0$. Moreover, $A \approx B$ abbreviates $A \lesssim B \lesssim A$.

For the analysis of a posteriori error estimation, two kinds of bubble functions are presented in [1], one associated with inner edges and the other with the point x_0. In this section these bubbles functions will be used and some of their properties will be quoted without proof.

Given $E \in \varepsilon_h$, let b_E be the bubble function defined in Ω, with support $\omega_E := \bigcup\{T \in \mathcal{T}_h : E \subset \partial T\}$ (see Figure 1), defined for $x \in \omega_E$ by

$$b_E(x) := \begin{cases} (\lambda_{P_2}^{T_1}\lambda_{P_3}^{T_1}\lambda_{P_2}^{T_2}\lambda_{P_3}^{T_2})^2 \dfrac{|x-x_0|^2}{|E|^2}, & \text{if } x_0 \in \omega_E^0, \\ (\lambda_{P_2}^{T_1}\lambda_{P_3}^{T_1}\lambda_{P_2}^{T_2}\lambda_{P_3}^{T_2})^2, & \text{otherwise}. \end{cases} \tag{2.1}$$

In this definition, the notations shown in Figure 1 are used. Moreover, ω_E^0 is the interior of ω_E, and $\lambda_{P_i}^{T_j}$ is the barycentric coordinate of x associated with the triangle T_j and the point P_i, which is extended to the whole ω_E.

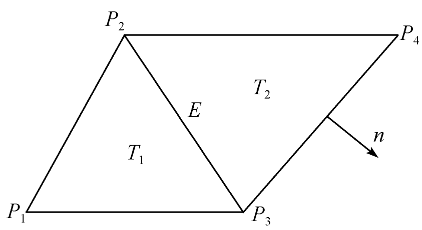

Figure 1 Support ω_E of b_E

Let $p, q \in (1,\infty)$ be a pair of conjugate numbers such that $\frac{1}{p} + \frac{1}{q} = 1$. Then there holds

Lemma 2.1.[1] *Given $E \in \varepsilon_h$, let b_E and ω_E be defined as above. Then*

$$\frac{\partial b_E}{\partial n} = 0, \qquad \text{on } \partial\omega_E, \tag{2.2}$$

$$\int_E b_E \approx h_E, \tag{2.3}$$

$$|b_E|_{m,q,\omega_E} \lesssim h_E^{2-m-2/p}, \qquad m = 1, 2. \tag{2.4}$$

Because in practice the meshes are usually constructed in such a way that x_0 is a vertex of all triangulation, x_0 is not a node of P_1 nonconforming finite elements. In this case, the definition of estimator will include an additional term (see (1.4) and (1.6)), another bubble function has to be used.

Let T_0 be a triangle of $\mathcal{T}_h$ containing x_0 (if x_0 lies on an inner edge, any of the two triangles sharing the edge can be chosen as T_0, and if x_0 is a vertex, any of the triangles sharing x_0 may be chosen as T_0). Denote $\omega_{T_0} := \bigcup\{T \in \mathcal{T}_h : T \cap T_0 \neq \emptyset\}$ and $d := \operatorname{dist}(x_0, \partial\omega_{T_0})$ (see Figure 2).

Notice that, because of the regularity of the mesh, $h_{T_0} \lesssim d$. Let b_{x_0} be a smooth bubble function defined in Ω , with support in ω_{T_0} and satisfying

$$0 \leqslant b_{x_0}(x) \leqslant 1, \qquad \forall x \in \Omega, \tag{2.5}$$

$$b_{x_0}(x) = 1, \qquad \forall x \in \Omega : |x - x_0| \leqslant \frac{d}{4}, \tag{2.6}$$

$$b_{x_0}(x) = 0, \qquad \forall x \in \Omega : |x - x_0| \geqslant \frac{3d}{4}, \tag{2.7}$$

$$|b_{x_0}|_{m,\infty,\omega_T} \lesssim d^{-m}, \qquad m = 1, 2. \tag{2.8}$$

Such a function can be easily obtained by convolution of the characteristic function of the set $\{x \in \Omega : |x - x_0| < d/4\}$ with a mollifier (see for instance [1]).

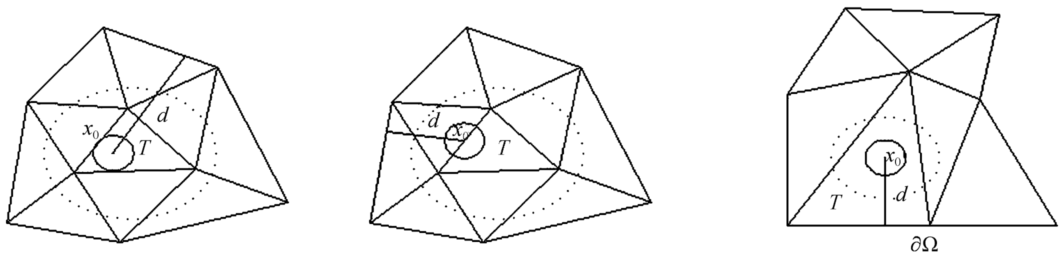

Figure 2 Domains ω_T for different locations of x_o. Circles $|x - x_0| = \frac{d}{4}$ (solid line) and $|x - x_0| = \frac{3d}{4}$ (dashed line)

Lemma 2.2.[1] *For $x_0 \in T_0$, Let b_{x_0} and ω_{T_0} be defined as above. Then*

$$|b_{x_0}|_{m,q,\omega_{T_0}} \lesssim h_{T_0}^{2-m-2/p}, m = 1, 2.$$

Furthermore, from Lemma 2.2, there holds

Lemma 2.3. *Let $x_0 \in T_0$ and ω_{T_0} be defined as above. Let $\mathcal{F}_h^{T_0}$ be the set of edges E of triangles $T \subset \omega_{T_0}$, such that E does not belong to $\partial\omega_{T_0}$. Then*

$$h_{T_0}^{2-p} \lesssim \sum_{T \in \omega_{T_0}} |u - u_h|_{1,p,T}^p + \sum_{E \in \mathcal{F}_h^{T_0}} \|h_E^{\frac{1}{p}} J_E(u_h)\|_{0,p,E}^p.$$

Proof. Let b_{x_0} be the bubble function defined above. By using (2.5), Green formula, Hölder inequality, Lemma 2.2, and the regularity of the mesh, there holds

$$\begin{aligned}
1 = \langle \delta_{x_0}, b_{x_0} \rangle &= \int_\Omega -\triangle u b_{x_0} = \int_{\omega_{T_0}} \nabla u \cdot \nabla b_{x_0} \\
&= \sum_{T \in \omega_{T_0}} \int_T \nabla_h (u - u_h) \cdot \nabla b_{x_0} + \sum_{T \in \omega_{T_0}} \int_T \nabla_h u_h \cdot \nabla b_{x_0} \\
&= \sum_{T \in \omega_{T_0}} \int_T \nabla_h (u - u_h) \cdot \nabla b_{x_0} + \sum_{T \in \omega_{T_0}} \int_{\partial T} \frac{\partial u_h}{\partial n} b_{x_0} \\
&= \sum_{T \in \omega_{T_0}} \int_T \nabla_h (u - u_h) \cdot \nabla b_{x_0} + \sum_{E \in \mathcal{F}_h^{T_0}} \int_E J_E(u_h) b_{x_0} \\
&\leqslant \Big(\sum_{T \in \omega_{T_0}} |u - u_h|_{1,p,T}^p \Big)^{\frac{1}{p}} |b_{x_0}|_{1,q,\omega_{T_0}} + \sum_{E \in \mathcal{F}_h^{T_0}} |J_E(u_h)| h_E \\
&\lesssim \Big(\sum_{T \in \omega_{T_0}} |u - u_h|_{1,p,T}^p \Big)^{\frac{1}{p}} h_{T_0}^{1-\frac{2}{p}} + \sum_{E \in \mathcal{F}_h^{T_0}} \|h_E^{\frac{1}{p}} J_E(u_h)\|_{0,p,E} h_{T_0}^{1-\frac{2}{p}},
\end{aligned}$$

which leads to the following estimate

$$h_{T_0}^{\frac{2}{p}-1} \lesssim \Big(\sum_{T\in\omega_{T_0}} |u-u_h|_{1,p,T}^p \Big)^{\frac{1}{p}} + \sum_{E\in\mathcal{F}_h^{T_0}} \|h_E^{\frac{1}{p}} J_E(u_h)\|_{0,p,E}. \tag{2.9}$$

The desired result follows from Hölder inequality and (2.9).

Let $v_h \in W_h$ be C^0-piecewise linear interpolation of a function $v \in \mathcal{C}(\Omega)$. Then we have

Lemma 2.4. *Given $E \in \varepsilon_h$, let ω_E be defined above. There holds:*

$$\begin{aligned} &\|v-v_h\|_{0,q,E} \lesssim h_E^{1+1/p}|v|_{2,q,\omega_E}, \quad \forall\, v\in W^{2,q}(\omega_E), \quad 1<q<\infty,\\ &\|v-v_h\|_{0,q,E} \lesssim h_E^{1/p}|v|_{1,q,\omega_E}, \quad \forall\, v\in W^{1,q}(\omega_E), \quad 2<q<\infty. \end{aligned}$$

Proof. Trace theorem, scaling arguments, and Hölder inequality lead to

$$\|v-v_h\|_{0,q,E} \lesssim h_E^{-\frac{1}{q}}\|v-v_h\|_{0,q,\omega_E} + h_E^{1-\frac{1}{q}}\Big(\sum_{T\in\omega_E}|v-v_h|_{1,q,T}^q\Big)^{\frac{1}{q}}. \tag{2.10}$$

Then the estimates of the lemma follow from (2.10) and the standard error estimates for the Lagrange interpolation (see for instance [11]),

$$\begin{aligned} |v-v_h|_{k,q,T} &\lesssim h_E^{2-k}|v|_{2,q,T}, \quad 1<q<\infty,\ k=0,1,\\ |v-v_h|_{k,q,T} &\lesssim h_E^{1-k}|v|_{1,q,T}, \quad 2<q<\infty,\ k=0,1. \end{aligned}$$

Lemma 2.5. *Given any interior edge $E\in\varepsilon_h$, let $\psi_E \in W_h$ be the edge-basis function with the support* supp $\psi_E \subset \overline{\omega_E}$ *and u_h the solution of the problem* (1.3). *Then there holds*:

$$[\nabla_h u_h]_E \cdot n_E = h_E^{-1}\langle \delta_{x_0}, \psi_E\rangle.$$

Proof. Since $[\nabla_h u_h]_E \cdot n_E \in P_0(E) \equiv R$, we have

$$h_E[\nabla_h u_h]_E \cdot n_E = ([\nabla_h u_h]_E, n_E)_{0,E} = ([\nabla_h u_h]_E\cdot n_E, \psi_E)_{0,E}.$$

Since ψ_E is L^2-orthogonal onto constants on all edges except E, $\mathrm{div}_h\nabla_h u_h = 0$ and ψ_E is an admissible test function for NFE Methods with support in $\overline{\omega_E}$, the application of Green's formula yields

$$\begin{aligned} ([\nabla_h u_h]_E\cdot n_E, \psi_E)_{0,E} &= (\nabla_h u_h\cdot n, \psi_E)_{0,\partial\omega_E} + ([\nabla_h u_h]_E\cdot n_E,\psi_E)_{0,E}\\ &= (\nabla_h u_h, \nabla_h\psi_E)_{0,\omega_E} + (\mathrm{div}_h\nabla_h u_h, \psi_E)_{0,\omega_E}\\ &= \langle \delta_{x_0}, \psi_E\rangle, \end{aligned}$$

which implies the desired result.

3 A posteriori error estimator in piecewise $W^{1,p}$ seminorm

Since the solution of (1.1) belongs to $W_0^{1,p}(\Omega)$ for all $p<2$, it makes sense to estimate the error in piecewise $W^{1,p}$ seminorm for the nonconforming method. In this section, the estimator ε_p in (1.4) is shown to be equivalent to the error $\|\nabla_h(u-u_h)\|_{0,p,\Omega}$ in (1.5) for any $p\in(p^\Omega,2)$, with $p^\Omega>1$ as shown below.

Given $\Psi \in L^q(\Omega)^2$, with $\frac{1}{p}+\frac{1}{q}=1$, consider the following problem: find $v \in W_0^{1,q}(\Omega)$ such that

$$\int_\Omega \nabla v \cdot \nabla \phi = \int_\Omega \Psi \cdot \nabla \phi, \qquad \forall\, \phi \in W_0^{1,p}(\Omega). \tag{3.1}$$

For any polygonal domain Ω, there exists a neighborhood of 2 such that, for all q in this neighborhood, the problem (3.1) has a unique solution v. Furthermore, in such a case, there holds the following estimate:

$$|v|_{1,q,\Omega} \leqslant C\|\Psi\|_{0,q,\Omega}. \tag{3.2}$$

To determine the range of values of q for which this holds true, we apply the arguments in the proof of Theorem 1.1 in [32] to the simpler two-dimensional Dirichlet problem (3.1). By doing so, we have to distinguish two cases, depending if Ω is convex or not. When Ω is convex, this happens for all $q \in (1,\infty)$ or, equivalently, for all $p \in (1,\infty)$. Instead, for a non-convex domain Ω, it happens if $1-2/q < \pi/\theta$, or equivalently, if $p > 2/(1+\frac{\pi}{\theta})$, with θ being the largest inner angle of Ω. Hence, if we define $p^\Omega := \max(1, 2/(1+\frac{\pi}{\theta}))$, then the problem (3.1) has a unique solution satisfying (3.2) for all $p \in (p^\Omega, 2)$.

For nonconforming triangular elements, as we know, the Helmholtz decomposition of the error is a well-established tool in the analysis of a posteriori estimate in piecewise H^1 seminorm (see e.g. [25, 30, 31]). Following the same idea, in this paper, to obtain the a posteriori error estimator in piecewise $W^{1,p}$ seminorm, we need the following Helmholtz-type decomposition of functions in $L^q(\Omega)^2$.

Lemma 3.1. *For $\Psi \in L^q(\Omega)^2$ with $\frac{1}{q}+\frac{1}{p}=1$ and $p \in (p^\Omega, 2)$, there exist $v \in W_0^{1,q}(\Omega)$, $w \in W^{1,q}(\Omega)$, such that*

$$\Psi = \nabla v + \mathrm{curl} w \tag{3.3}$$

with

$$|v|_{1,q,\Omega} \lesssim \|\Psi\|_{0,q,\Omega}, \qquad |w|_{1,q,\Omega} \lesssim \|\Psi\|_{0,q,\Omega}. \tag{3.4}$$

Proof. Let v be the solution of the Dirichlet problem (3.1). From (3.1) and integration by parts, we have

$$\begin{aligned} 0 = \int_\Omega (\Psi - \nabla v)\cdot \nabla \phi &= \int_\Omega -\mathrm{div}(\Psi-\nabla v)\phi + \int_{\partial\Omega} (\Psi - \nabla v)\cdot \boldsymbol{n}\phi \\ &= \int_\Omega -\mathrm{div}(\Psi - \nabla v)\phi, \quad \forall \phi \in W_0^{1,p}(\Omega). \end{aligned}$$

This implies $\Psi - \nabla v$ is divergence-free. Moreover, from integration by parts, we get

$$\int_{\partial\Omega} (\Psi - \nabla v)\cdot \boldsymbol{n} ds = 0. \tag{3.5}$$

Thus $\Psi - \nabla v$ satisfies the conditions of Theorem 3.1 in [33] on the polygonal domain Ω, namely it is divergence-free and fulfills (3.5). As a result, there exists $w \in W^{1,q}(\Omega)$ such that

$$\nabla v - \Psi = \mathrm{curl} w, \tag{3.6}$$

which implies (3.3).

The desired regularity estimates in (3.4) follow from (3.2), (3.6) and triangle inequalities.

Now we are in a position to state the reliability of the estimator ε_p:

Theorem 3.1. *Let $u_h \in W_h$ solve the problem* (1.3) *and ε_p be defined as in* (1.4)*. Then the following estimate holds for $p \in (p^\Omega, 2)$:*

$$\|\nabla_h(u-u_h)\|_{0,p,\Omega} \lesssim \varepsilon_p.$$

Proof. Arbitrarily given $\Psi \in L^q(\Omega)^2$, with $\frac{1}{p}+\frac{1}{q}=1$. From Lemma 3.1, there exist $v \in W_0^{1,q}(\Omega)$, $w \in W^{1,q}(\Omega)$ satisfying (3.3). Then we have

$$\int_\Omega \nabla_h(u-u_h)\cdot\Psi = \int_\Omega \nabla_h(u-u_h)\cdot\nabla v + \int_\Omega \nabla_h(u-u_h)\cdot \mathrm{curl} w. \tag{3.7}$$

Let v_h be C^0-piecewise linear interpolation of v in the nonconforming finite element space W_h. Green formula, together with (1.3), implies

$$\begin{aligned}\int_\Omega \nabla_h(u-u_h)\cdot\nabla v &= \int_\Omega \nabla u\cdot\nabla v - \sum_{T\in\mathcal{T}_h}\int_T \nabla_h u_h\cdot\nabla v\\ &= \int_\Omega -\triangle u(v-v_h) + \sum_{T\in\mathcal{T}_h}\int_T \nabla_h u_h\cdot\nabla_h(v_h-v)\\ &= \langle\delta_{x_0}, v-v_h\rangle + \sum_{T\in\mathcal{T}_h}\int_T \nabla_h u_h\cdot\nabla_h(v_h-v)\\ &= \langle\delta_{x_0}, v-v_h\rangle + \sum_{T\in\mathcal{T}_h}\int_{\partial T} \frac{\partial u_h}{\partial \boldsymbol{n}}(v_h-v)\\ &= \langle\delta_{x_0}, v-v_h\rangle + \sum_{E\in\varepsilon_h}\int_E [\nabla_h u_h]_E\cdot\boldsymbol{n}_E(v_h-v).\end{aligned} \tag{3.8}$$

Let w_h be C^0-piecewise linear interpolation of w on the triangulation $\mathcal{T}_h$, then, from integration by parts and the fact that $w \in W^{1,q}(\Omega) \hookrightarrow C^0(\Omega)$, we have

$$\begin{aligned}\int_\Omega \nabla_h(u-u_h)\cdot\mathrm{curl} w &= \int_\Omega \nabla u\cdot\mathrm{curl} w - \int_\Omega \nabla_h u_h\cdot\mathrm{curl} w\\ &= -\int_\Omega \nabla_h u_h\cdot\mathrm{curl}(w-w_h) - \int_\Omega \nabla_h u_h\cdot\mathrm{curl} w_h.\end{aligned} \tag{3.9}$$

Since $w_h \in C^0(\Omega)$, the tangential derivative $\frac{\partial w_h}{\partial s}$ of w_h is a constant along every inner edge. Note also that u_h is continuous at the midpoint of every interior edge, and vanishes at the midpoint of every boundary edge, from integration by parts, we then have

$$\int_\Omega \nabla_h u_h\cdot\mathrm{curl} w_h = \sum_{T\in\mathcal{T}_h}\int_T \nabla_h u_h\cdot\mathrm{curl} w_h = -\sum_{T\in\mathcal{T}_h}\int_{\partial T}\nabla w_h\cdot\tau u_h = 0. \tag{3.10}$$

From (3.9), (3.10), and integration by parts, we have

$$\begin{aligned}\int_\Omega \nabla_h(u-u_h)\cdot\mathrm{curl} w &= -\sum_{T\in\mathcal{T}_h}\int_T \nabla_h u_h\cdot\mathrm{curl}(w-w_h)\\ &= -\sum_{T\in\mathcal{T}_h}\int_{\partial T}\frac{\partial u_h}{\partial s}(w-w_h)\end{aligned}$$

$$= -\sum_{E\in\varepsilon}\int_E [\nabla_h u_h]_E \cdot \tau_E (w - w_h), \tag{3.11}$$

where, for $E \subset \partial\Omega$, $[\nabla_h u_h]_E \cdot \tau_E = \nabla_h u_h \cdot \tau_E = \frac{\partial u_h}{\partial s}$.

From the definition of $\int_\Omega v_h \delta_{x_0}$ in Section 1 and the standard interpolation theory (see [11]), we get

$$\int_\Omega (v-v_h)\delta_{x_0} = \frac{1}{k}\sum_{i=1}^{k}(v-v_h)|_{T0i}(x_0) \leqslant \frac{1}{k}\sum_{i=1}^{k}\|v-v_h\|_{0,\infty,T_{0i}} \lesssim \frac{1}{k}\sum_{i=1}^{k} h_{T_{0i}}^{1-\frac{2}{q}}|v|_{1,q,T_{0i}}, \tag{3.12}$$

where T_{0i} $(1 \leqslant i \leqslant k)$ denote the triangles sharing the point x_0.

In the case that $E \subset \partial\Omega$ with $E \subset \partial T$ and $T \in \mathcal{T}_h$, we have $\omega_E = T$. By (3.7), (3.8), (3.11), (3.12), Hölder inequality, standard interpolation theory, Lemmas 2.4, and 3.1, we obtain

$$\begin{aligned}\int_\Omega \nabla_h(u-u_h)\cdot\Psi \lesssim\ & \frac{1}{k}\sum_{i=1}^{k} h_{T_{0i}}^{1-\frac{2}{q}}|v|_{1,q,T_{0i}} \\ &+ \sum_{E\in\varepsilon_h}\|[\nabla_h u_h]_E\cdot\boldsymbol{n}_E\|_{0,p,E}\|(v_h - v)\|_{0,q,E} \\ &+ \sum_{E\in\varepsilon}\|[\nabla_h u_h]_E\cdot\tau_E\|_{0,p,E}\|(w-w_h)\|_{0,q,E} \\ \lesssim\ & \frac{1}{k}\sum_{i=1}^{k} h_{T_{0i}}^{1-\frac{2}{q}}|v|_{1,q,T_{0i}} + \sum_{E\in\varepsilon_h}\|h_E^{\frac{1}{p}}[\nabla_h u_h]_E\cdot\boldsymbol{n}_E\|_{0,p,E}|v|_{1,q,\omega_E} \\ &+ \sum_{E\in\varepsilon}\|h_E^{\frac{1}{p}}[\nabla_h u_h]_E\cdot\tau_E\|_{0,p,E}|w|_{1,q,E} \\ \lesssim\ & \Bigg(\sum_{i=1}^{k}\frac{h_{T_{0i}}^{2-p}}{k^p} + \sum_{E\in\varepsilon_h}\|h_E^{\frac{1}{p}}[\nabla_h u_h]_E\|_{0,p,E}^p \\ &+ \sum_{E\subset\partial\Omega}\left\|h_E^{\frac{1}{p}}\frac{\partial u_h}{\partial s}\right\|_{0,p,E}^p\Bigg)^{\frac{1}{p}}\Bigg(\sum_{E\in\varepsilon}|v|_{1,q,\omega_E}^q + |w|_{1,q,\omega_E}^q\Bigg)^{\frac{1}{q}} \\ \lesssim\ & \varepsilon_p\|\Psi\|_{0,q,\Omega},\end{aligned}$$

which indicates

$$\|\nabla_h(u-u_h)\|_{0,p,\Omega} = \sup_{\Psi\in L^q(\Omega)^2,\Psi\neq 0}\frac{\int_\Omega \nabla_h(u-u_h)\cdot\Psi}{\|\Psi\|_{0,q,\Omega}} \lesssim \varepsilon_p. \tag{3.13}$$

Then the desired result follows from (3.13).

Next we give the following efficiency result of the estimator ε_p:

Theorem 3.2. *Let $u_h \in W_h$ solve the problem* (1.3). *Then the following estimate holds for $p \in (p^\Omega, 2)$:*

$$\varepsilon_p \lesssim \|\nabla_h(u-u_h)\|_{0,p,\Omega}.$$

Proof. For all $E \in \varepsilon_h(\Omega)$, let b_E be the bubble function defined in Section 2. Since $b_E \in W_0^{1,q}(\Omega)$, from Green formula, we have

$$\begin{aligned}\int_{\omega_E}\nabla_h u_h\cdot\nabla b_E &= \sum_{T\in\omega_E}\int_T \nabla_h u_h\cdot\nabla b_E = \sum_{T\in\omega_E}\int_{\partial T}[\nabla_h u_h]_E\cdot \boldsymbol{n}_E b_E\\ &= \int_E [\nabla_h u_h]_E\cdot\boldsymbol{n}_E b_E,\end{aligned}\tag{3.14}$$

which, together with (2.2), the relation $\int_\Omega -\triangle u b_E = 0$ and Green formula, yields

$$\begin{aligned}\int_E [\nabla_h u_h]_E\cdot\boldsymbol{n}_E b_E &= \int_{\omega_E}\nabla_h u_h\cdot\nabla b_E = \int_{\omega_E}\nabla_h u_h\cdot\nabla b_E - \int_\Omega -\triangle u b_E\\ &= \int_{\omega_E}\nabla_h u_h\cdot\nabla b_E - \int_\Omega \nabla u\cdot\nabla b_E = \sum_{T\in\mathcal{T}_h}\int_T \nabla_h(u_h-u)\cdot\nabla b_E\\ &= \sum_{T\in\omega_E}\int_T\nabla_h(u_h-u)\cdot\nabla b_E.\end{aligned}\tag{3.15}$$

On the other hand, from (2.3), (2.4), (3.15), Hölder inequality, and Cauchy-Schwartz inequality, we also have

$$\begin{aligned}h_E|[\nabla_h u_h]_E\cdot\boldsymbol{n}_E| &\lesssim |[\nabla_h u_h]_E\cdot\boldsymbol{n}_E|\int_E b_E = \left|\int_E[\nabla_h u_h]_E\cdot\boldsymbol{n}_E b_E\right|\\ &= \left|\sum_{T\in\omega_E}\int_T\nabla_h(u_h-u)\cdot\nabla b_E\right|\\ &\lesssim \left(\sum_{T\in\omega_E}|u-u_h|_{1,p,T}^p\right)^{\frac1p}\left(\sum_{T\in\omega_E}|b_E|_{1,q,T}^q\right)^{\frac1q}\\ &\lesssim \left(\sum_{T\in\omega_E}|u-u_h|_{1,p,T}^p\right)^{\frac1p} h_E^{1-\frac2p}.\end{aligned}\tag{3.16}$$

The inequality (3.16) implies

$$\|h_E^{\frac1p}[\nabla_h u_h]_E\cdot\boldsymbol{n}_E\|_{0,p,E}\lesssim\left(\sum_{T\in\omega_E}|u-u_h|_{1,p,T}^p\right)^{\frac1p}.\tag{3.17}$$

From Lemma 2.3, we get

$$\begin{aligned}\sum_{i=1}^k\frac{h_{T_{0i}}^{2-p}}{k^p} &\lesssim \sum_{i=1}^k\left(\frac{1}{k^p}\sum_{T\in\omega_{T_{0i}}}|u-u_h|_{1,p,T}^p+\frac{1}{k^p}\sum_{E\in\mathcal{F}_h^{T_{0i}}}\left\|h_E^{\frac1p}\left[\frac{\partial u_h}{\partial\boldsymbol{n}_E}\right]\right\|_{0,p,E}^p\right)\\ &\leqslant \frac1k\sum_{i=1}^k\left(\sum_{T\in\omega_{T_{0i}}}|u-u_h|_{1,p,T}^p+\sum_{E\in\mathcal{F}_h^{T_{0i}}}\|h_E^{\frac1p}[\nabla_h u_h]_E\cdot\boldsymbol{n}_E\|_{0,p,E}^p\right).\end{aligned}\tag{3.18}$$

For arbitrary $E\in\varepsilon_h$, shared by the elements T_+ and T_-, by connecting the midpoint $\mathrm{mid}(E)$ with the vertices of T_+ and T_- opposite to it, We can divide T_+ and T_- into triangles T_1, T_2 and T_3, T_4, respectively.

Let φ_E be a multiple of the conforming P_1 FEM basis function with respect to the nodal point $\mathrm{mid}(E)$ such that

$$\varphi_E(\mathrm{mid}(E)) = h_E^2\ |[\nabla_h u_h]_E\cdot\tau_E|\ [\nabla_h u_h]_E\cdot\tau_E.$$

From Hölder inequality, we have

$$\|\overrightarrow{\mathrm{curl}\varphi_E}\|_{0,q,\omega_E}^q \approx \int_{\omega_E} |\overrightarrow{\mathrm{curl}\varphi_E}|^q \lesssim \sum_{j=1}^{4}\sum_{i=1}^{2} \|D_i\varphi_E\|_{0,q,T_j}^q.$$

Notice that $\|D_i\varphi_E\|_{0,q,T_j}^q \lesssim h_E^{2-q}|\varphi_E(\mathrm{mid}(E))|^q$, from the above inequality we have

$$\|\overrightarrow{\mathrm{curl}\varphi_E}\|_{0,q,\omega_E} \lesssim h_E^{1+\frac{1}{q}}\|[\nabla_h u_h]_E\cdot\tau_E\|_{0,p,E}^{p-1}|[\nabla_h u_h]_E\cdot\tau_E|^{3-p}. \tag{3.19}$$

Because the segmentwise tangential derivative $\partial\varphi_E/\partial s$ of φ_E vanishes along $\partial\omega_E$, by using integration by parts, we get

$$\begin{aligned} &h_E^2\|[\nabla_h u_h]_E\cdot\tau_E\|_{0,p,E}^p|[\nabla_h u_h]_E\cdot\tau_E|^{3-p} \\ &= h_E^{\frac{1}{p}}\|[\nabla_h u_h]_E\cdot\tau_E\|_{0,p,E}^p h_E^{1+\frac{1}{q}}|[\nabla_h u_h]_E\cdot\tau_E|^{3-p} \\ &= \int_E \varphi_E[\nabla_h u_h]_E\cdot\tau_E = \int_{\omega_E}\overrightarrow{\mathrm{curl}\varphi_E}\cdot\nabla_h u_h. \end{aligned} \tag{3.20}$$

From integration by parts, we also have

$$\int_{\omega_E}\overrightarrow{\mathrm{curl}\varphi_E}\cdot\nabla u = \int_{\partial\omega_E}(\partial\varphi_E/\partial s)u = 0. \tag{3.21}$$

The above two identities, (3.20) and (3.21), and Hölder inequality imply

$$\begin{aligned} &h_E^{\frac{1}{p}}\|[\nabla_h u_h]_E\cdot\tau_E\|_{0,p,E}^p h_E^{1+\frac{1}{q}}|[\nabla_h u_h]_E\cdot\tau_E|^{3-p} \\ &= \int_{\omega_E}\overrightarrow{\mathrm{curl}\varphi_E}\cdot(\nabla_h u_h-\nabla u) \leqslant \|\overrightarrow{\mathrm{curl}\varphi_E}\|_{0,q,\omega_E}\|\nabla_h u_h-\nabla u\|_{0,p,\omega_E}. \end{aligned} \tag{3.22}$$

Combination of (3.22) and (3.19) yields the inequality

$$h_E^{\frac{1}{p}}\|[\nabla_h u_h]_E\cdot\tau_E\|_{0,p,E} \lesssim \|\nabla_h u_h-\nabla u\|_{0,p,\omega_E}. \tag{3.23}$$

In the case that $E\subset\partial\Omega$ with $E\subset\partial T$, $T\in\mathcal{T}_h$, by using $u|_E=0$ to substitute for the segmentwise tangential derivative of φ_E which does not vanish along the two components of the boundary edge E, and by following the same proof as above, we can also obtain (3.23).

For any $E\in\varepsilon_h$, by Hölder inequality, we have

$$\begin{aligned} h_E\|[\nabla_h u_h]_E\|_{0,p,E}^p &\approx h_E\int_E(|[\nabla_h u_h]_E\cdot\boldsymbol{n}_E|^2+|[\nabla_h u_h]_E\cdot\tau_E|^2)^{\frac{p}{2}} \\ &\lesssim h_E\left(\int_E|[\nabla_h u_h]_E\cdot\boldsymbol{n}_E|^p+\int_E|[\nabla_h u_h]_E\cdot\tau_E|^p\right) \\ &= h_E\|[\nabla_h u_h]_E\cdot\boldsymbol{n}_E\|_{0,p,E}^p + h_E\|[\nabla_h u_h]_E\cdot\tau_E\|_{o,p,E}^p. \end{aligned} \tag{3.24}$$

Because every element in summation $\sum_{i=1}^k\sum_{T\in\omega_{T_{0i}}}$ is used at most k times repeatedly, and every inner edge in $\sum_{i=1}^k\sum_{E\in\mathcal{F}_h^{T_{0i}}}$ is also used at most k times repeatedly, from (3.17), (3.18), (3.23), and (3.24), we get

$$\varepsilon_p^p \lesssim \sum_{T\in\mathcal{T}_h}|u-u_h|_{1,p,T}^p.$$

Then the desired result follows.

Remark 3.1. The proofs of Theorems 3.1 and 3.2 are still valid when x_0 is a node of the triangulation or an interior point of an element. In fact, in this case, the term $\langle \delta_{x_0}, v - v_h \rangle$ vanishes and thus the term $\sum_{i=1}^{k} \frac{h_{T_{0i}}^{2-p}}{k^p}$ does not appear in ε_p.

Remark 3.2. When Ω is convex, according to the definition of p^Ω, ($p^\Omega = 1$). Hence, in this case, the estimator ε_p turns out to be equivalent to $\|\nabla_h (u - u_h)\|_{0,p,\Omega}$ for all $p \in (1, 2)$.

4 A global upper bound for the error in L^p norm

In this section, we will prove that the estimator η_p in (1.6) is a global upper bound for the error $\|u - u_h\|_{0,p,\Omega}$ ($\frac{2\theta}{\pi} < p < 2$), with θ the largest inner angle of Ω. In the proof of Theorem 4.1 below we will use duality arguments. To this end we consider the following auxiliary problem:

$$\begin{cases} -\triangle v = \psi, & \text{in } \Omega, \\ v = 0, & \text{on } \partial\Omega, \end{cases} \tag{4.1}$$

where $\psi \in L^q(\Omega)$ and $\frac{1}{p} + \frac{1}{q} = 1$. According to Theorem 4.4 in [34], if

$$\left(2 - \frac{\pi}{\theta}\right) q < 2, \tag{4.2}$$

then the solution of (4.1) satisfies $v \in W^{2,q}(\Omega)$ and

$$|v|_{2,q,\Omega} \lesssim \|\psi\|_{0,q,\Omega}. \tag{4.3}$$

In the case that Ω is a triangle with three acute angles or a rectangle, $\theta \leqslant \frac{\pi}{2}$ and (4.3) holds true for all $q < \infty$. In other cases, the largest angle of Ω satisfies $\theta > \frac{\pi}{2}$ and, consequently, (4.3) holds true only for $q < 2/(2 - \frac{\pi}{\theta})$ or, equivalently, for $p > \frac{2\theta}{\pi}$. Denote $p_\Omega := \max\{1, \frac{2\theta}{\pi}\}$, then, for $p \in (p_\Omega, 2)$, the inequality (4.3) holds.

Theorem 4.1. *For $p \in (p_\Omega, 2)$, let $u_h \in W_h$ solve the problem* (1.3)*, and η_p be defined as in* (1.6)*. Then the following estimate holds*:

$$\|u - u_h\|_{0,p,\Omega} \lesssim \eta_p.$$

Proof. Given $\psi \in L^q(\Omega)$, let $v \in W^{2,q}(\Omega)$ be the solution of (4.1), and let $v_h \in W_h$ be C^0-piecewise linear interpolation of v. From (1.3), integration by parts and Sobolev imbedding theorem, we have

$$\begin{aligned} \int_\Omega (u - u_h)\psi &= \int_\Omega -\triangle v (u - u_h) = \int_\Omega \nabla v \cdot \nabla u - \int_\Omega -\triangle v u_h \\ &= \int_\Omega -\triangle u v - \sum_{T \in \mathcal{T}_h} \int_T \nabla v \cdot \nabla_h u_h + \sum_{T \in \mathcal{T}_h} \int_{\partial T} \frac{\partial v}{\partial \boldsymbol{n}} u_h \\ &= \int_\Omega -\triangle u (v - v_h) + \int_\Omega -\triangle u v_h - \sum_{T \in \mathcal{T}_h} \int_{\partial T} \frac{\partial u_h}{\partial \boldsymbol{n}} v + \sum_{T \in \mathcal{T}_h} \int_{\partial T} \frac{\partial v}{\partial \boldsymbol{n}} u_h \\ &= \int_\Omega -\triangle u (v - v_h) + \sum_{T \in \mathcal{T}_h} \int_T \nabla u_h \cdot \nabla v_h - \sum_{T \in \mathcal{T}_h} \int_{\partial T} \frac{\partial u_h}{\partial \boldsymbol{n}} v + \sum_{T \in \mathcal{T}_h} \int_{\partial T} \frac{\partial v}{\partial \boldsymbol{n}} u_h \\ &= \langle \delta_{x_0}, v - v_h \rangle + \sum_{T \in \mathcal{T}_h} \int_{\partial T} \frac{\partial u_h}{\partial \boldsymbol{n}} (v_h - v) + \sum_{T \in \mathcal{T}_h} \int_{\partial T} \frac{\partial v}{\partial \boldsymbol{n}} u_h \end{aligned}$$

$$= \frac{1}{k}\sum_{i=1}^{k}(v-v_h)|_{T0i}(x_0) + \sum_{E\in\varepsilon_h}\int_E J_E(u_h)(v_h-v)$$
$$+ \sum_{E\in\varepsilon_h}\int_E \frac{\partial v}{\partial \boldsymbol{n}_E}[u_h]_E + \sum_{E\subset\partial\Omega}\int_E \frac{\partial v}{\partial \boldsymbol{n}_E}u_h. \tag{4.4}$$

For arbitrary interior edge $E\in\varepsilon_h$ shared by the triangles T_+ and T_-, let ω_E be the patch of E, and denote $\alpha_E := \frac{1}{|\omega_E|}\int_{\omega_E}\nabla v dx$. By Schwartz inequality, trace theorem, Hölder inequality, Bramble-Hilbert lemma, we have

$$\begin{aligned}\|\nabla v-\alpha_E\|_{0,q,E} &\leqslant \|\nabla v-\alpha_E\|_{0,q,\partial T_+} + \|\nabla v-\alpha_E\|_{0,q,\partial T_-}\\ &\lesssim \|\nabla v-\alpha_E\|_{0,q,T_+}^{1-\frac{1}{q}}\|\nabla v-\alpha_E\|_{1,q,T_+}^{\frac{1}{q}}\\ &\quad + \|\nabla v-\alpha_E\|_{0,q,T_-}^{1-\frac{1}{q}}\|\nabla v-\alpha_E\|_{1,q,T_-}^{\frac{1}{q}}\\ &\leqslant (\|\nabla v-\alpha_E\|_{0,q,T_+} + \|\nabla v-\alpha_E\|_{0,q,T_-})^{\frac{1}{p}}\\ &\quad \times (\|\nabla v-\alpha_E\|_{1,q,T_+} + \|\nabla v-\alpha_E\|_{1,q,T_-})^{\frac{1}{q}}\\ &\lesssim \|\nabla v-\alpha_E\|_{0,q,\omega_E}^{\frac{1}{p}}\|\nabla v-\alpha_E\|_{1,q,\omega_E}^{\frac{1}{q}}\\ &\lesssim (h_E|\nabla v|_{1,q,\omega_E})^{\frac{1}{p}}|\nabla v|_{1,q,\omega_E}^{\frac{1}{q}} = h_E^{\frac{1}{p}}|v|_{2,q,\omega_E}.\end{aligned} \tag{4.5}$$

In the case that $E\subset\partial\Omega$ with $E\subset\partial T$, we have $\omega_E = T$ and $\alpha_E = \frac{1}{|T|}\int_T \nabla v dx$. By using an analogous argument, we have

$$\|\nabla v-\alpha_E\|_{0,q,E} \lesssim h_E^{\frac{1}{p}}|v|_{2,q,\omega_E}. \tag{4.6}$$

Since $E\subset\partial\Omega$, from the relation $\frac{1}{h_E}\int_E u_h ds = 0$ and Bramble-Hilbert lemma, we have

$$\|u_h\|_{0,p,E} = \left\|u_h - \frac{1}{h_E}\int_E u_h ds\right\|_{0,p,E} \lesssim h_E\|\partial_\varepsilon u_h\|_{0,p,E}, \tag{4.7}$$

which, together with (4.5), (4.6), Hölder inequality, and $\int_E [u_h]_E ds = 0$, indicates

$$\begin{aligned}&\sum_{E\in\varepsilon_h}\int_E \frac{\partial v}{\partial \boldsymbol{n}_E}[u_h]_E + \sum_{E\subset\partial\Omega}\int_E \frac{\partial v}{\partial \boldsymbol{n}_E}u_h\\ &\quad = \sum_{E\in\varepsilon_h}\int_E(\nabla v-\alpha_E)\cdot\boldsymbol{n}_E[u_h]_E + \sum_{E\subset\partial\Omega}\int_E(\nabla v-\alpha_E)\cdot\boldsymbol{n}_E u_h\\ &\quad \lesssim \sum_{E\in\varepsilon_h}\|\nabla v-\alpha_E\|_{0,q,E}\|[u_h]_E\|_{0,p,E} + \sum_{E\subset\partial\Omega}\|\nabla v-\alpha_E\|_{0,q,E}\|u_h\|_{0,p,E}\\ &\quad \lesssim \sum_{E\in\varepsilon_h} h_E^{\frac{1}{p}}|v|_{2,q,\omega_E}\|[u_h]_E\|_{0,p,E} + \sum_{E\subset\partial\Omega} h_E^{1+\frac{1}{p}}|v|_{2,q,\omega_E}\|\partial_\varepsilon u_h\|_{0,p,E}.\end{aligned} \tag{4.8}$$

By using standard interpolation theory, Hölder inequality, Lemma 2.4, (4.3), (4.4), and (4.8), we have

$$\begin{aligned}\int_\Omega (u-u_h)\psi &\leqslant \frac{1}{k}\sum_{i=1}^{k}\|v-v_h\|_{0,\infty,T_{0i}} + \sum_{E\in\varepsilon_h}\|J_E(u_h)\|_{0,p,E}\|v_h-v\|_{0,q,E}\\ &\quad + \left(\sum_{E\in\varepsilon_h} h_E^{\frac{1}{p}}\|[u_h]_E\|_{0,p,E} + \sum_{E\subset\partial\Omega} h_E^{1+\frac{1}{p}}\|\partial_\varepsilon u_h\|_{0,p,E}\right)|v|_{2,q,\omega_E}\end{aligned}$$

$$
\begin{aligned}
&\lesssim \frac{1}{k}\sum_{i=1}^{k} h_{T_{0i}}^{2-\frac{2}{q}}|v|_{2,q,T_{0i}} + \sum_{E\in\varepsilon_h}\|J_E(u_h)\|_{0,p,E}h_E^{1+\frac{1}{p}}|v|_{2,q,\omega_E} \\
&\quad + \left(\sum_{E\in\varepsilon_h} h_E^{\frac{1}{p}}\|[u_h]_E\|_{0,p,E} + \sum_{E\subset\partial\Omega} h_E^{1+\frac{1}{p}}\|\partial_\varepsilon u_h\|_{0,p,E}\right)|v|_{2,q,\omega_E} \\
&\lesssim \left\{\sum_{i=1}^{k}\frac{h_{T_{0i}}^2}{k^p} + \sum_{E\in\varepsilon_h}(\|J_E(u_h)\|_{0,p,E}^p h_E^{p+1} + h_E\|[u_h]_E\|_{0,p,E}^p)\right. \\
&\quad \left. + \sum_{E\subset\partial\Omega} h_E^{1+p}\|\partial_\varepsilon u_h\|_{0,p,E}^p\right\}^{\frac{1}{p}} \\
&\quad \times\left\{\left(\sum_{E\in\varepsilon_h} + \sum_{E\subset\partial\Omega}\right)|v|_{2,q,\omega_E}^q + \sum_{i=1}^{k}|v|_{2,q,T_{0i}}^q\right\}^{\frac{1}{q}} \\
&\lesssim \left\{\sum_{i=1}^{k}\frac{h_{T_{0i}}^2}{k^p} + \sum_{E\in\varepsilon_h}|J_E(u_h)|^p h_E^{p+2} + \sum_{E\in\varepsilon_h} h_E\|[u_h]_E\|_{0,p,E}^p\right. \\
&\quad \left. + \sum_{E\subset\partial\Omega} h_E^{1+p}\|\partial_\varepsilon u_h\|_{0,p,E}^p\right\}^{\frac{1}{p}}\|\psi\|_{0,q,\Omega}, \qquad (4.9)
\end{aligned}
$$

which yields

$$
\|u-u_h\|_{0,p,\Omega} = \sup_{\psi\in L^q(\Omega),\psi\neq 0}\frac{\int_\Omega (u-u_h)\psi}{\|\psi\|_{0,q,\Omega}} \lesssim \eta_p.
$$

Remark 4.1. The proof of the theorem 4.1 also remains valid when x_0 is a node of the triangulation. Indeed, in this case, the term $\langle \delta_{x_0}, v - v_h\rangle$ vanishes and thus the term $\sum_{i=1}^{k}\frac{h_{T_{0i}}^2}{k^p}$ does not appear in η_p .

Remark 4.2. From Lemma 2.5, we know that for $E \in \varepsilon_h$, $J_E(u_h) = 0$ when $E \not\subseteq \omega_{x_0}$. Then the term $\sum_{E\in\varepsilon_h} h_E^{p+2}|J_E(u_h)|^p$ in the estimator η_p can be reduced to $\sum_{E\in\varepsilon_h, E\subset\omega_{x_0}} h_E^{p+2}|J_E(u_h)|^p$.

5 Numerical experiments

In this section we report several numerical experiments to asses the performance of an h-adaptive mesh-refinement strategy based on the error indicators ε_p and η_p analyzed in sections 3 and 4.

The adaptive procedure consists in solving the problem (1) on a sequence of meshes up to finally attaining a solution with an estimated error within a prescribed tolerance. It invokes that the solution of the finite element discretized problem (3) (SOLVE), the a posteriori error estimation of the global discretization error (ESTIMATE) by easily computable local quantities as an indication to mark selected elements (MARK) for refinement, and the refinement strategy (REFINE) itself. Thus, Adaptive finite element methods typically consist of successive loops of the sequence

SOLVE → ESTIMATE → MARK → REFINE.

For this purpose, we initiate the process with a quasi-uniform mesh and create, at each step, a new mesh better adapted to the solution of the problem (1). Let M_k and M_h denote the sets of the marked triangles and edges, respectively. Denote

$$
\varepsilon_E^p = \begin{cases} \|h_E^{\frac{1}{p}}[\nabla_h u_h]_E\|_{0,p,E}^p, & \text{for all } E\in\varepsilon_h, \\ \|h_E^{\frac{1}{p}}\nabla_h u_h\cdot\tau_E\|_{0,p,E}^p, & \text{for all } E\subset\partial\Omega, \end{cases}
$$

and

$$\eta_E^p = \begin{cases} h_E^{p+2}|J_E(u_h)|^p + h_E\|[u_h]_E\|_{0,p,E}^p, & \text{for all } E \in \varepsilon_h, \\ h_E^{1+p}\|\partial_\varepsilon u_h\|_{0,p,E}^p, & \text{for all } E \subset \partial\Omega. \end{cases}$$

The adaptive procedure is done by computing the global error indicator η_p or ε_p in the "old" mesh $\mathcal{T}_h$, and marking those elements T and edges E with

$$\begin{cases} \displaystyle\sum_{T_{0i}\in M_k} h_{T_{0i}}^2 \geqslant \theta \sum_{i=1}^k h_{T_{0i}}^2, \\ \displaystyle\sum_{E\in M_h} \eta_E^p \geqslant \theta \sum_{E\in\varepsilon} \eta_E^p, \end{cases}$$

or

$$\begin{cases} \displaystyle\sum_{T_{0i}\in M_k} h_{T_{0i}}^{2-p} \geqslant \theta \sum_{i=1}^k h_{T_{0i}}^{2-p}, \\ \displaystyle\sum_{E\in M_h} \varepsilon_E^p \geqslant \theta \sum_{E\in\varepsilon} \varepsilon_E^p, \end{cases}$$

where, $\theta \in (0,1)$ is a prescribed parameter. Thus, combination of M_h and the longest edge of all the elements in M_k forms the edge set to be refined (see [14]). In the REFINE step, we use the longest-edge bisection (see [19–22]). In all our experiments we take $\theta = \frac{1}{2}$, and use a Matlab code adapted by us with an initial uniform mesh.

The Laplace equation with homogeneous Dirichlet boundary conditions serves as a model example in this paper for the ease of the discussion. Similar to [24, 26], we can extend Theorems 3.1 and 4.1 to nonhomogeneous boundary cases, where the estimators will contain a higher order term related to the approximation error of the Dirichlet data u_D.

5.1 Test 1: a convex domain

This test for the error estimators η_p and ε_p consists of solving the problem $-\triangle u = \delta_{x_0}$ in the unit square $\Omega := (0,1)\times(0,1)$, with $x_0 = (0.5, 0.5)$. We choose Dirichlet boundary conditions such that the exact solution is given by $u = -\frac{1}{2\pi}\log|x - x_0|$.

We show first the results obtained by the adaptive process guided by the estimator η_p. Figures 3–5 show some of the successive refined meshes created in the process guided by η_p

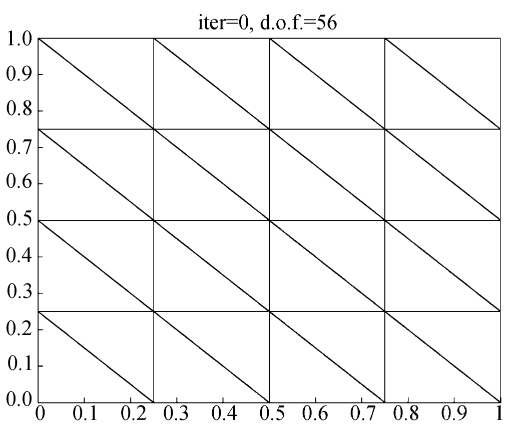

Figure 3

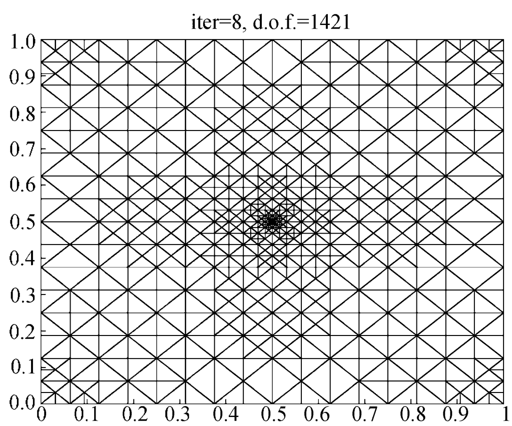

Figure 4

with $p = 1.5$, where x_0 is a vertex of all the triangulations. Figures 6–8 show the post-processing approximate solution, with value at a vertex being taken as the algorithmic mean of the values of the nonconforming finite element solution u_h at the vertex on all the elements sharing the vertex. The reason for the post-processing is that u_h is not continuous at all the vertices of the triangulation. Figures 3–8 also show the iteration number and the number of degrees of freedom (d.o.f.) of each mesh. Figure 9 shows the error curves of the whole process for the exact, estimated and uniformly refined errors. This figure also includes a line with slope-1, which corresponds to the theoretically optimal order of convergence for piecewise linear elements. From Figures 3–5, we can see that the adaptive process leads to meshes refined around x_0. Furthermore, the error curves in Figure 9 shows that the process yields optimal order convergence. This happens in spite of the fact that the effectivity indices are very poor. Indeed, we can see in Figure 9 that the exact error is severely overestimated. Anyway, the exact and estimated error curves have approximately the same optimal slope-1, and the adaptive process has obvious advantages than the uniform refinements.

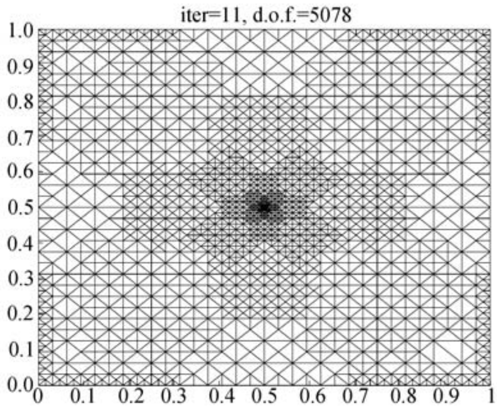

Figure 5

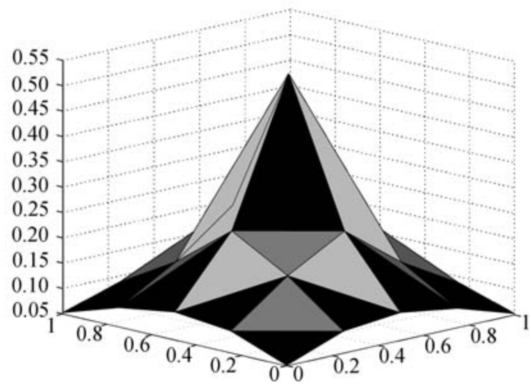

Figure 6

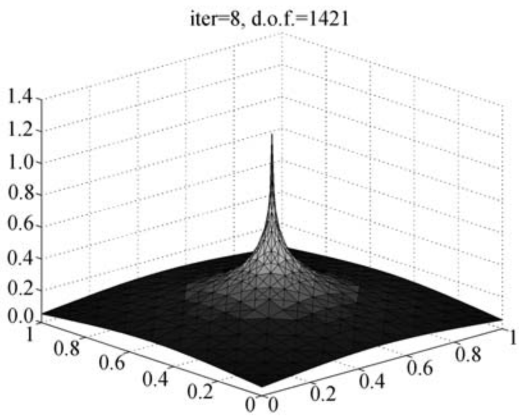

Figure 7

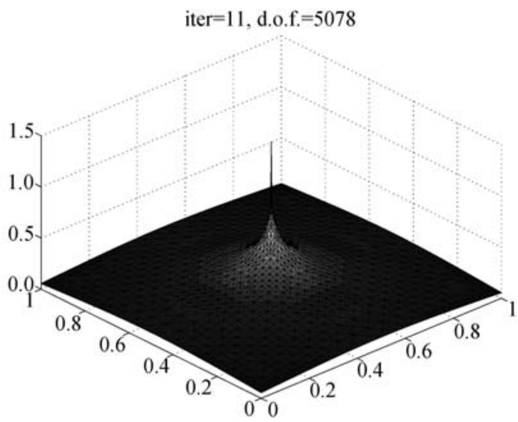

Figure 8

Next, we report the results obtained with ε_p as error indicator. Figures 10–12 show some of the successively refined meshes created with the adaptive process guided by this indicator with $p = 1.5$ and x_0 being a vertex of the triangulations, Figures 13–15 show the post-processing

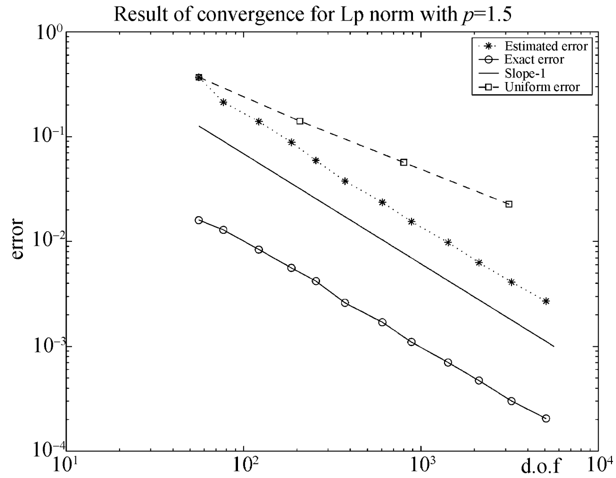

Figure 9

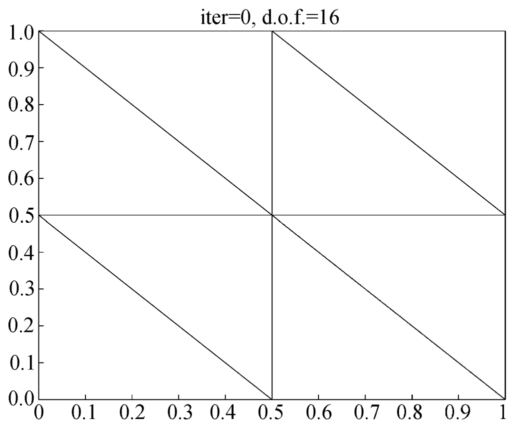

Figure 10

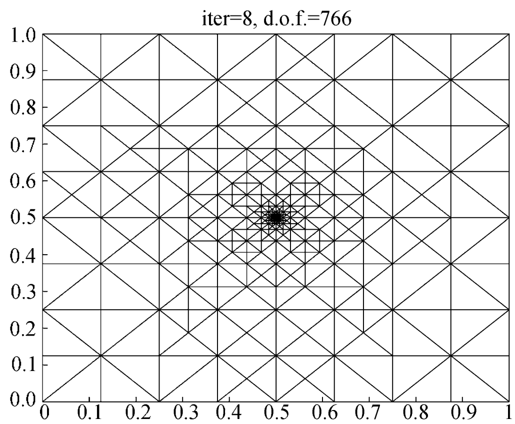

Figure 11

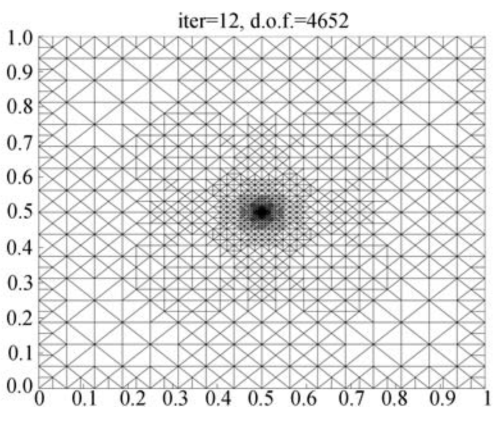

Figure 12

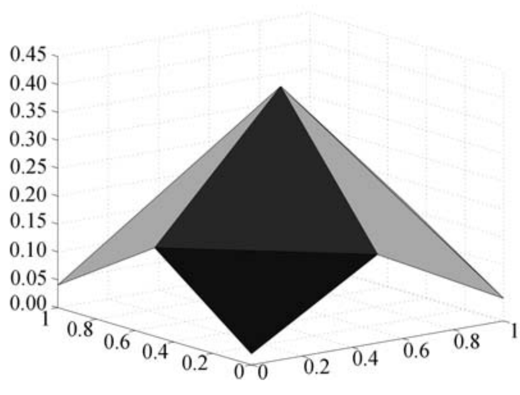

Figure 13

approximate solution, and Figures 10–15 also show the iteration number, and the number of degrees of freedom (d.o.f.) of each mesh.

Figure 16 shows the error curves for the exact and estimated errors. It also includes a line with slope $-\frac{1}{2}$, which corresponds to the theoretically optimal order of convergence for piecewise linear elements in problems with a smooth solution.

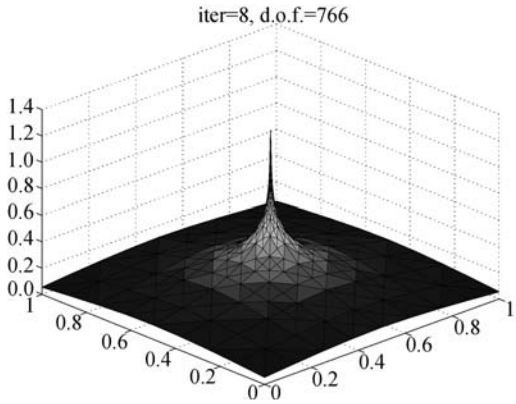

Figure 14

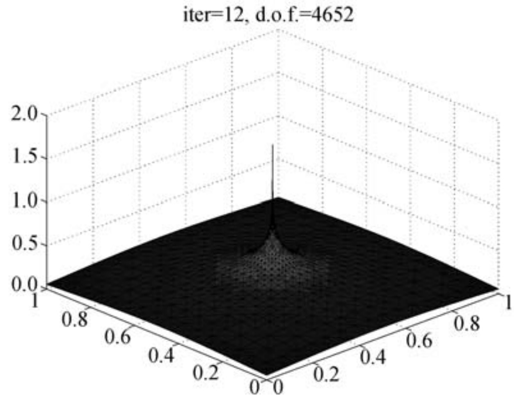

Figure 15

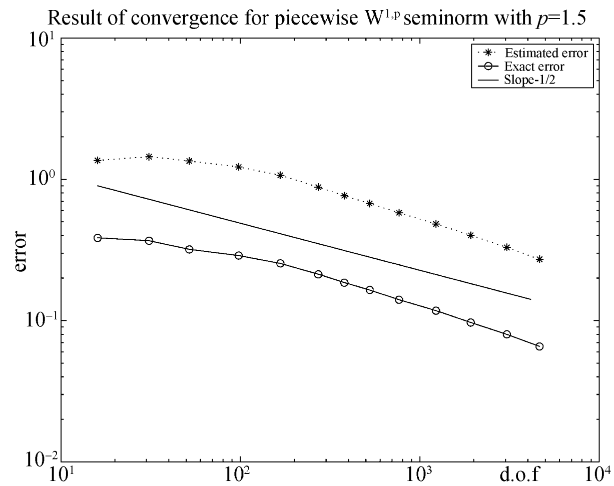

Figure 16

Figures 10–12 show that the adaptive process leads again to meshes refined around x_0.

5.2 Test 2: a non-convex domain

We solve the problem $-\triangle u = \delta_{x_0}$ in the L-shape domain shown in Figure 17. We choose Dirichlet boundary conditions such that the exact solution be $u(x,y) = u_1(x,y) + u_2(x,y)$, where

$$u_1(x,y) = -\frac{1}{2\pi}\log|x - x_0| \quad \text{and} \quad u_2(x,y) = r^{\frac{2}{3}}\sin\left(\frac{2}{3}\theta\right).$$

Here (r,θ) are the polar coordinates corresponding to (x,y) with $\theta \in [0,2\pi)$. Recall that u_2 is the typical singular solution of the Dirichlet problem for this L-shape domain.

We use ε_p with $p = 1.5$ to measure the error. Notice that $u \in W^{1,p}(\Omega)$ for all $p \in [1,2)$. Moreover, Theorem 3.1 can be applied to this case, because, according to the definition of p^Ω, $p^\Omega = \frac{6}{5}$ for this particular domain. However Theorem 4.1 is not applicable to L^p norm, because, according the definition of p_Ω, $p_\Omega = 3$ for this domain.

Figures 18–20 show some of the successively refined meshes created in the adaptive process guided by ε_p, with $p = 1.5$. We can see that the adaptive process leads to meshes refined around both x_0 and the corner singularity.

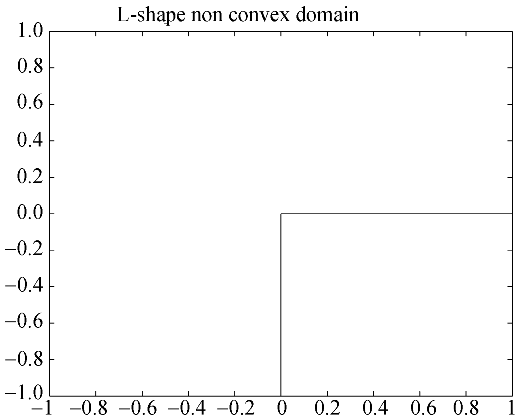

Figure 17

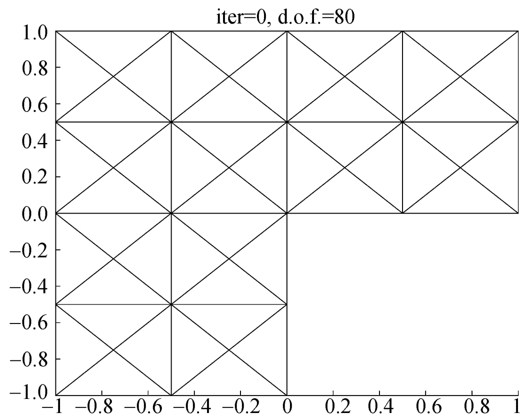

Figure 18

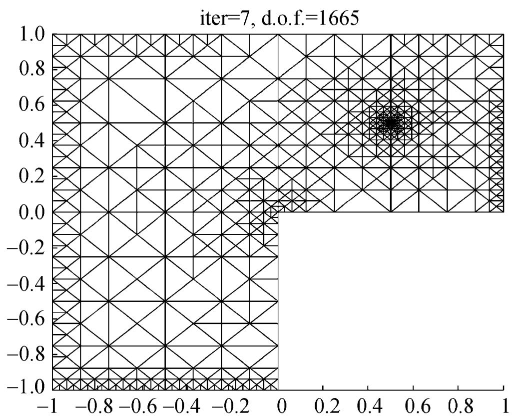

Figure 19

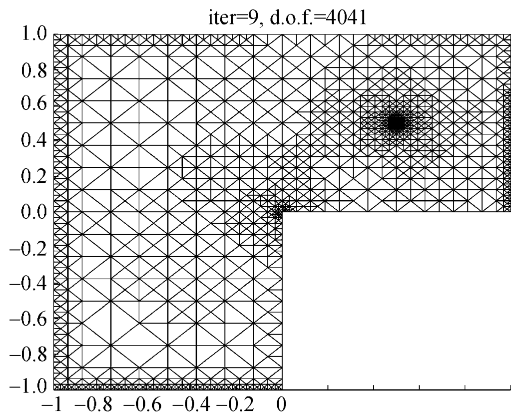

Figure 20

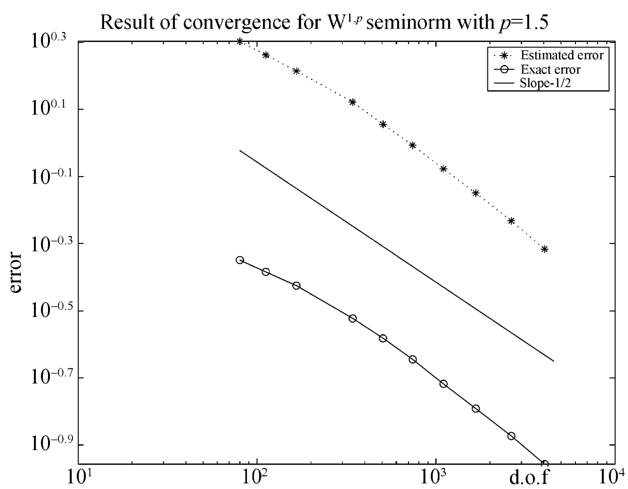

Figure 21

On the other hand, Figure 21 shows the corresponding exact and estimated error curves. Once more, we can see that the adaptive process yields optimal order convergence: both of the exact and estimated error curves have approximately the same optimal slope $-\frac{1}{2}$.

6 Conclusions

We have introduced two residual-based type a posteriori error estimators for the nonconforming finite element approximation of the Poisson problem with Dirac delta source terms. We have shown that one estimator yields a global upper and lower bounds of the error in piecewise $W^{1,p}$ seminorm, and the other gives a global upper bound in L^p norm. Adaptive algorithms are suggested and experimentally shown to lead to optimal orders of convergence.

Acknowledgements The authors are very grateful to Prof. Xu Xuejun for his helpful suggestions.

References

1 Araya R, Behrens E, Rodríguez R. A posteriori error estimates for problems with Dirac delta source terms. *Numer Math*, **105**: 193–216 (2006)
2 Casas E. L^2 estimates for the finite element method for the Dirichlet problem with singular data. *Numer Math*, **47**: 627–632 (1985)
3 Scott R. Finite element convergence for singular data. *Numer Math*, **21**: 317–327 (1973/74)
4 Schatz A H, Wahlbin L B. Interior maximum norm estimtes for finite element methods. *Math Comp*, **31**: 414–442 (1977)
5 Chen Z, Dai S. Adaptive Galerkin methods with error control for a dynamical Ginzburg-Landau model in superconductivity. *SIAM J Numer Anal*, **38**: 1961–1985 (2001)
6 Chen Z, Dai S. On the efficiency of adaptive finite methods for elliptic problems with discontinuous coefficients. *SIAM J Sci Comput*, **24**: 443–462 (2002)
7 Hoppe W, Wohlmuth B. Element-oriented and edge-oriented local error estimators for nonconforming finite element methods. *RAIRO Model Math Anal Numer*, **30**: 237–263 (1996)
8 Dari E, Duran R G, Padra C, Vampa V. A posteriori error estimators for nonconforming finite element methods. *RAIRO Model Math Anal Numer*, **30**: 385–400 (1996)
9 Schieweck F. A posteriori error estimates with post-processing for nonconforming finite elements. *ESAIM Math Mod Numer Anal*, **36**: 489–503 (2002)
10 Carstensen C, Hu J. A unifying theory of a posteriori error control for nonconforming finite element methods. *Numer Math*, **107**: 473–502 (2007)
11 Ciarlet P G. The Finite Element Method for Elliptic Problems. Amsterdam: Nort-Holland, 1978
12 Braess D. Finite Elements. Cambridge: Cambridge University Press, 1977
13 Brenner S, ScottL R. The Mathematical Theory of Finite Element Methods. New York: Springer, 1994
14 Carstensen C, Ronald H, Hoppe W. Convergence analysis of an adaptive nonconforming finite element method. *Numer Math*, **105**: 251–266 (2006)
15 Bartels S, Carstensen C, Dolzmann G. Inhomogeneous Dirichlet conditions in a priori and a posteriori finite element error analysis. *Numer Math*, **99**: 1–24 (2004)
16 Binev P, Dahmen W, DeVore R. Adaptive finite element methods with convergence rates. *Numer Math*, **97**: 219–268 (2004)
17 Dörfler W. A convergent adaptive algorithm for Poisson's equation. *SIAM J Numer Anal*, **33**: 1106–1124 (1996)
18 Morin P, Nochetto R H, Siebert K G. Data oscillation and convergence of adaptive FEM. *SIAM J Numer Anal*, **38**: 466–488 (2000)
19 Rivara M C. Mesh refinement processes based on the generalized bisection of simplices. *SIAM J Numer Anal*, **21**: 604–613 (1984)
20 Rivara M C, Inostroza P. Using longest-side bisection techniques for the automatic refinement for Delaunay triangulations. *Intern J Nume Methods Engineering*, **40**: 581–597 (1997)
21 Rivara M C, Iribarren G. The 4-triangles longest-side partition of triangles and linear refinement algorithms. *Math Comput*, **65**: 1485–1501 (1996)
22 Rivara M C, Venere M. Cost analysis of the longest-side (triangle bisection) refinement algorithms for triangulations. *Engineering with Computers*, **12**: 224–234 (1996)
23 Babuška I, Rheinboldt W C. Error estimates for adaptive finite element computations. *SIAM J Numer Anal*, **15**: 736–754 (1978)

24 Carstenson C, Bartels S. Each averaging technique yields reliable a posteriori error control in FEM on unstructured grids. Part one: low order conforming, nonconforming, and mixed FEM. *Math Comput*, **71**: 945–969 (2002)

25 Carstensen C, Bartels S, Jansche S. A posteriori error estimates for nonconforming finite element methods. *Numer Math*, **92**: 233–256 (2002)

26 Carstensen C, Hu J, Orlando A. Framework for the a posteriori error analysis of nonconforming finite elements. *SIAM J Numer Anal*, **45**: 68–82 (2007)

27 Eriksson K, Estep D, Hansbo P, Johnson C. Introduction to adaptive methods for differential equations. *Acta Numer*, **4**: 105–158 (1995)

28 Morin P, Nochetto R H, Siebert K G. Local problems on stars: a posteriori error estimators, convergence, and performance. *Math Comput*, **72**: 1067–1097 (2002)

29 Verfürth R. A review of a posteriori error estimation and adaptive mesh-refinement techniques. Wiley-Teubner, 1996

30 Anisworth M. A synthesis of a posteriori error estimation techniques for conforming, non-conforming and discontinuous Galerkin finite element methods. *Contemp Math*, **383**: 1–14 (2005)

31 Anisworth M. Robust a posteriori error estimation for conforming, nonconforming finite element approximation. *SIAM J Numer Anal*, **42**: 2320–2341 (2005)

32 Dauge M. Neumann and mixed problems on curvilinear polyhedra. *Integral Equations Oper Theory*, **15**: 227–261 (1992)

33 Girault P, Raviart P A. Finite Element Methods for Navier-Stokes Equations. Berlin: Springer, 1986

34 Grisvard P. Elliptic problems for non-smooth domains. Boston: Pitman, 1985